

Radioheliograph Observations of Microwave Bursts with Zebra Structures

A.T. Altyntsev¹ · S.V. Lesovoi¹ ·
N.S. Meshalkina¹ · R.A. Sych^{2,1} · Y. Yan²

© Springer

Abstract The so-called zebra structures in radio dynamic spectra, specifically their frequencies and frequency drifts of emission stripes, contain information on the plasma parameters in the coronal part of flare loops. This paper presents observations of zebra structures in a microwave range. Dynamic spectra were recorded by Chinese spectro-polarimeters in the frequency band close to the working frequencies of the Siberian Solar Radio Telescope. The emission sources are localized in the flare regions, and we are able to estimate the plasma parameters in the generation sites using X-ray data. The interpretation of the zebra structures in terms of the existing theories is discussed. The conclusion has been arrived that the preferred generation mechanism of zebra structures in the microwave range is the conversion of plasma waves to electromagnetic emission on the double plasma resonance surfaces distributed across a flare loop.

Keywords: Solar flares; Radio bursts; Microwave emission; Dynamic spectrum; Zebra pattern

1. Introduction

Narrow-band structures in the dynamic spectra of radio bursts have attracted much attention from solar radio astronomers. Their coherent emission is generated by a nonthermal electron component, and its characteristics may be used to determine the plasma parameters in flare regions close to the site of their initial energy release. The most remarkable among these structures is the so-called zebra structure observed in the dynamic spectra as several, concurrently changing stripes of higher emission intensity.

The frequencies of the zebra emission must be above the cutoff frequency that is the Langmuir frequency in the source. Structures in meter- and decimeter-wave ranges are generated in low-density plasmas in the upper corona at heights

¹Institute of Solar-Terrestrial Physics SB RAS, Lermontov
St. 126A, Irkutsk 664033, Russia email: altyntsev@iszf.irk.ru

² Key Laboratory of Solar Activity, National Astronomical
Observatories, CAS, Beijing 100012, China e-mail:
yyh@bao.ac.cn

over several tens of thousands of kilometers (*e.g.*, see Chernov, 2006). In this case, a large number of stripes drifting to low frequencies are regularly observed. The sources of coherent emission at frequencies above 3 GHz should be located in dense plasma loops in the low corona. Zebra structures can rarely be seen in this frequency range. Among two hundred events with sub-second pulses recorded by the Siberian Solar Radio Telescope (SSRT, Grechnev *et al.*, 2003) and given in the catalogues (<http://badary.iszf.irk.ru/Ftevents.php> and <http://ssrt.iszf.irk.ru/fast>), we found only six flares with zebra structures observed in the dynamic spectra recorded with Chinese spectro-polarimeters (Fu *et al.*, 1995; Ji *et al.*, 2003).

The generation of coherent narrow-band bursts in the microwave range is associated with two-stage plasma mechanisms. At first, electrostatic plasma oscillations are excited. Then a part of the oscillation energy is converted into electromagnetic waves at frequencies close to the Langmuir frequency or to its harmonics. First of all, the zebra events with stripe frequencies divisible by the electron gyro-frequency were detected in the microwave range.

The frequency structure can be explained by the excitation of the Bernstein modes in compact homogeneous sources (Altyntsev *et al.*, 2005). The interpretation of events found later required other models because, as opposed to the Bernstein modes, the difference between the frequencies of adjacent stripes was not constant or was too small in comparison to the independent estimations of the cyclotron frequency. To explain such structures, Chernov *et al.* (2006) suggested, like the case for low-frequency zebra structures, that the emission of bright stripes is generated in some compact sources distributed along a flare loop. Here the emission frequency of a single strip is determined by the values of plasma density and magnetic field in its source.

Chernov *et al.* (2006) attributed the narrow-band emission to the excitation of upper hybrid $f_{\text{up}} = \sqrt{f_p^2 + f_B^2}$ and whistler waves $f_w < f_B$ by nonthermal electrons with a loss-cone velocity distribution. Here $f_p = \sqrt{\frac{ne^2}{\pi m}}$ is the Langmuir frequency and $f_B = \frac{eB}{2\pi mc}$ is the electron gyro-frequency. It is assumed that both types of plasma oscillation are excited simultaneously by the same population of nonthermal electrons. Plasma waves are converted into high-frequency electromagnetic waves when they merge together: $f = f_{\text{up}} + f_w$. As the whistler frequency f_w is low, the frequency of the electromagnetic wave f is close to the upper hybrid one.

Note that the closeness of the electromagnetic wave frequency to the Langmuir frequency results in its rapid damping in the plasma surrounding the source (Benz *et al.*, 1992). The most controversial point in the model of Chernov *et al.* (2006) is the assumption that the appearance of a number of quasi-harmonic stripes is due to discrete distribution of whistler-wave sources along a flare loop.

Zlotnik (2011) pointed out that the intensity of the electromagnetic emission does not depend considerably on the level T_w of low-frequency whistler turbulence. This conclusion follows from the Manley-Rowe relation: $T = \frac{f T_{\text{up}} T_w}{f_{\text{up}} T_w + f_w T_{\text{up}}}$. It is evident that at $f_{\text{up}} \gg f_w$ the brightness temperature of the electromagnetic emission is $T \cong T_{\text{up}}$. Hence, to explain the discrete distribution of radio sources, we should assume a discrete distribution of regions with upper-hybrid oscillation turbulence. The high-frequency plasma turbulence is expected to be

enhanced in compact regions in which the condition for double plasma resonance (DPR) $f_{\text{up}} = sf_B$ is fulfilled, where s is an integer (Zlotnik *et al.*, 2003; Kuznetsov and Tsap, 2007; Kuznetsov, 2008).

The observed characteristics of a multiple-strip zebra structure in the meter-wave range have been interpreted as due to the emission sources on the DPR surfaces (Aurass *et al.*, 2003; Zlotnik *et al.*, 2003). By comparing the frequencies of zebra stripes and the calculated values of gyro-frequency along the loop, the authors managed to obtain the plasma density as a function of height. It proved to be close to the expected hydrostatic distribution at a reasonable coronal plasma temperature of about 1 million degrees.

This paper discusses the observations of microwave zebra structures whose dynamic spectra were recorded by the spectro-polarimeters of Chinese observatories in a frequency range of 5.2–7.6 GHz comprising the receiving frequency of SSRT (5.7 GHz). The observational techniques will be described in Section 2. Using the SSRT interferometer observations, we were able to localize the microwave sources in the flare area and thus independently estimate the plasma parameters in the generation region using X-ray data. Section 3 will describe the observations of zebra structures. Section 4 is concerned with the applicability of the DPR mechanism to the interpretation of the generation of the zebra structure.

2. Instrumentation

The techniques for the observation of zebra structures have been described by Altyntsev *et al.* (2005). The dynamic spectra of zebra structures were observed with the Solar Radio Broadband Fast Dynamic Spectrometers (5.2–7.6 GHz, both circular polarizations, frequency and time resolution of 20 MHz and 5 ms, respectively) at the Huairou Solar Observing Station of the National Astronomical Observatories of China (NAOC) and the Purple Mountain Observatory (4.5–7.5 GHz, only intensity, 10 MHz, 5 ms) (Fu *et al.*, 1995; Ji *et al.*, 2003).

The spatial structure of the microwave sources was recorded by the Siberian Solar Radio Telescope (SSRT) (Grechnev *et al.*, 2003). Our investigation of the flare bursts with high time resolution are based on the data recorded by the EW and NS arrays, which simultaneously provide one-dimensional images (scans) of the solar disk every 14 ms. The analysis methods for one-dimensional solar images have been described by Altyntsev *et al.* (1996, 2003) and Lesovoi and Kardapolova (2003). The receiver system of SSRT contains a spectrum analyzer with 120 MHz frequency coverage using an acousto-optic detector with 250 frequency channels, which correspond to the knife-edge-shaped fan beams for the NS and EW arrays. The frequency channel bandwidth is 0.52 MHz. The response at each frequency corresponds to the emission from a narrow strip on the solar disk whose position and width depend on the observation time, array type, and frequency. The signals from all the channels are recorded simultaneously and generate a one-dimensional distribution of solar radio brightness. Each of the right and left components of circular polarization is recorded successively within the intervals of 7 ms. The minimal width of the beam of SSRT is 15'' and depends on the array direction and the local time of observation.

The data from Nobeyama Radioheliograph (Nakajima *et al.*, 1994), Nobeyama Radio Polarimeters (NoRP; Nakajima *et al.*, 1985; Torii *et al.*, 1979), and Radio Solar Telescope Network (RSTN) have been used to examine spatial and spectral characteristics of background microwave bursts. The data from *Reuven Ramaty High Energy Solar Spectroscopic Imager* (RHESSI) have been exploited to analyze X-rays from the nonthermal plasma component (Lin *et al.*, 2002). Some events have been studied using UV images of flares acquired by the *Transition Region and Coronal Explorer* (TRACE, Handy *et al.*, 1999). The magnetic field structure of flares was inferred from the Michelson Doppler Imager (MDI) magnetograms (Scherrer *et al.*, 1995).

3. Observations

Figure 1 presents the dynamic spectrum with a simple, two-stripe zebra structure. This structure was recorded at the Huairou station at the maximum of a short-duration microwave burst from a 17 September 2002 solar flare. The small flare of GOES X-ray class C2.0 occurred in AR 10114 (S12W42). The microwave burst with the maximum intensity of 60 sfu at 4 GHz lasted for less than one minute. Its spectrum shape was typical of the gyro-synchrotron emission. The simulation of the gyro-synchrotron spectrum (Ramaty, 1969; Ramaty *et al.*, 1994) shows that the magnetic field in the emission source was weaker than 200 gauss (G).

Narrow-band structures in the frequency range of 5.2–7.6 GHz were observed near the burst maximum for 5 s from 05:51:19 to 05:51:24 UT. Among them, on the continuous background spectrum, we can single out two zebras of about 1 s duration with a similar structure and separated by 3 s. Figure 1 shows the dynamic spectrum of the first structure. Two parallel stripes can be identified which drifted to higher frequencies at a rate of about 1 GHz s^{-1} initially, and later to lower frequencies at a rate of 1.8 GHz s^{-1} . The total bandwidth of this emission slightly exceeded 1 GHz. The turnover in the drifting rate took place in the high-frequency branch by $\Delta t = 85 \text{ ms}$ later than in the low-frequency one. The bandwidths of the emission branches are 0.15 GHz (ascending branch) and 0.23 GHz (descending one), and they are separated by 0.44 and 0.5 GHz, respectively.

During the flare, the interferometric observations at 17 GHz showed a loop with bright footpoints separated by $25''$ (Figure 2). At the footpoints were compact X-ray sources with emission at 25–50 keV. One-dimensional radio brightness distributions recorded by the EW and NS linear arms of SSRT at the frequency of 5.7 GHz indicated that the background burst source covered the entire flare loop at 17 GHz. As illustrated in Figure 1, the lower-frequency stripe of the zebra structure was emitted in the band of the SSRT operating frequencies. The emission amplitude of the zebra stripes did not exceed several solar flux units, and its sources in the ascending and descending branches were located at the top of the loop when the observation was made at 5.7 GHz. The relative displacement between the sources of different branches was within the accuracy of measurements of the centroid positions of radio brightness and was no more than $3''$ in the plane of the sky.

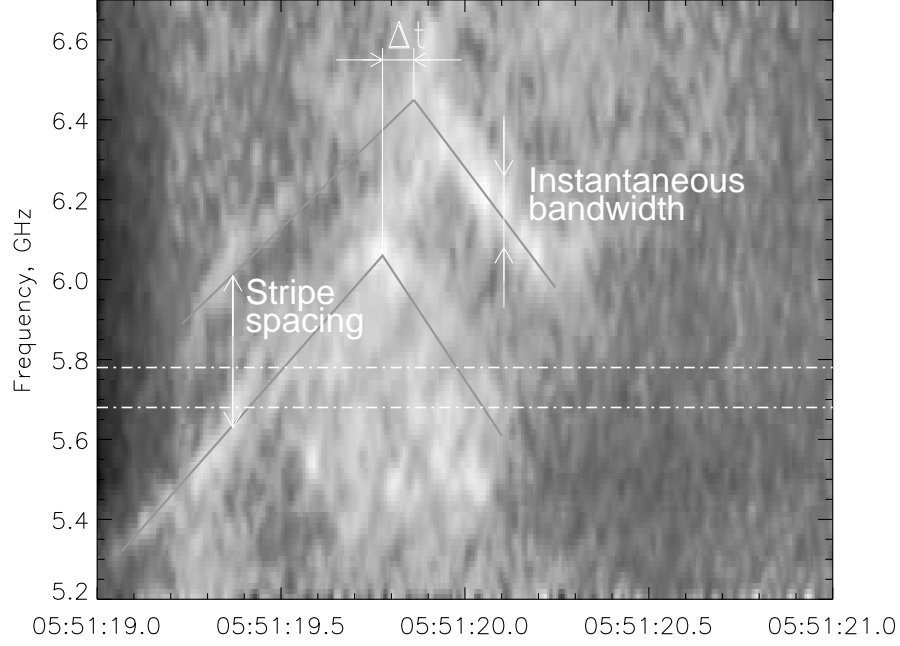


Figure 1. The dynamic spectrum of the zebra structure observed on 17 September 2002. White means increased emission. The zebra stripes are indicated by the grey lines. The horizontal lines mark the boundaries of the SSRT receiver bands.

A UV image of the flare at 195 \AA was available in a minute after the zebra structure was recorded. The total area of the flare brightening including the loop was about $4 \times 10^{17} \text{ cm}^2$. The GOES total flux observations show that the zebra structures were observed during the ascending phase of the emission measure at the constant temperature of $\approx 8 \text{ MK}$. From the emission measure of $2 \times 10^{47} \text{ cm}^{-3}$ follows the plasma density of $\approx 7 \times 10^{10} \text{ cm}^{-3}$, if we assume the thickness of the emitting region to be 10^8 cm .

Figure 3 presents the microwave dynamic spectrum recorded during the 29 May 2003 solar flare (Sych *et al.*, 2010). This event was distinguished by the presence of several zebra structures with three stripes (I, II, IV) and complex ones with four stripes (III, V). The short burst with the main phase of only $\approx 20 \text{ s}$ (02:13:00 – 02:13:20 UT) was associated with the flare of GOES class M1.5/1F (02:09 – 02:24 UT) in NOAA 10368 (S37E03). The zebra structures were observed at the maximum of the background burst whose emission was as much as 180 sfu at 9.4 GHz.

The left-hand-side panels of Figure 3 show the zebra structures expanded in time. The intensity of the stripes was within several solar flux units. The stripes with various frequency patterns and different drift rates were seen in a wide frequency range (5.8–7.2 GHz) for 4 s. Pulses with sub-second duration were recorded by the SSRT only during some structures: II (6), III (7), IV (7, 8). Note that a very rare event was recorded in which zebra stripes with different

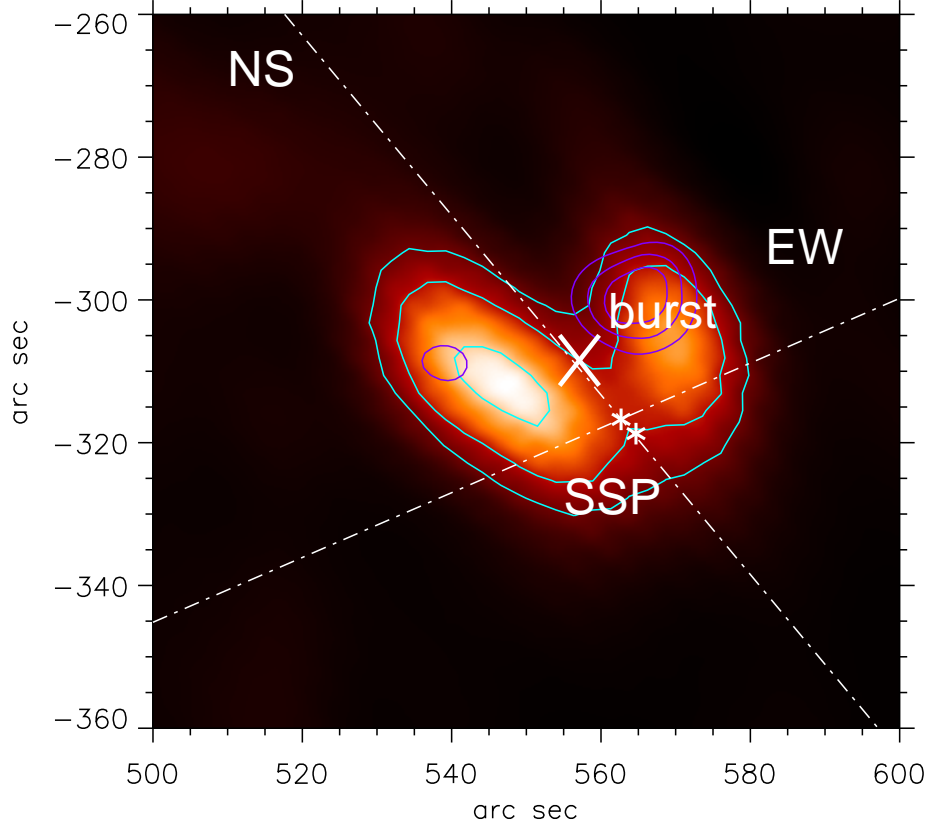


Figure 2. The configuration of the 17 September 2002 flare loop. The background image and blue contours at $[0.3, 0.5, 0.9] \times 0.2$ MK show the brightness temperature at the frequency of 17 GHz (05:51:23 UT). The purple contours indicate X-ray counts in the energy range of 25 to 50 keV integrated from 05:50:40 to 05:51:40 UT. The dash-dotted lines show the scan directions of the SSRT linear interferometers. The big cross marks the center of the radio burst source at 5.7 GHz, and the asterisks indicate the sources of the zebra structures. The source of the descending branch in Figure 1 is more distant from the center of the burst.

slopes were observed simultaneously (III, IV). Probably, two independent sources (two loops or two footpoints of the loop) were in the antenna beam.

The drifts were largely directed to higher frequencies. In the second and fifth intervals, the frequency drift was $df/dt = 1.3\text{--}1.5$ GHz s $^{-1}$ at a frequency splitting of 200 to 300 MHz between the stripes. In the first and third cases, $df/dt = 3.2\text{--}3.6$ GHz s $^{-1}$ at $\Delta f = 150\text{--}300$ MHz. From approximately 02:13:03.3 UT, two distinct and almost non-drifting stripes separated by 300 MHz appeared between 5.8–6.4 GHz.

In this event the zebra patterns demonstrated the so-called superfine temporal structure, namely the individual bright stripes were consisted of clusters of separate short-duration pulses (Sych *et al.*, 2010). Their duration and bandwidth were around the instrumental resolutions of 5 ms and 70–100 MHz, respectively.

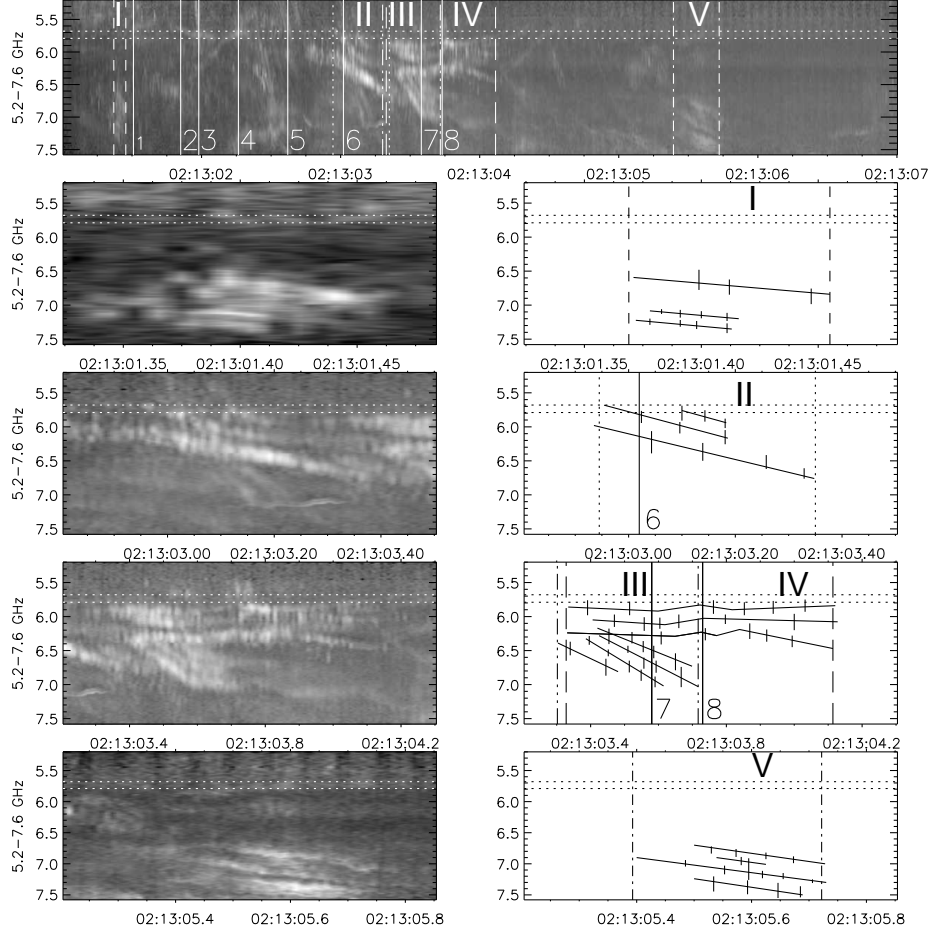


Figure 3. The dynamic spectra with fine structures observed on 29 May 2003 (top panel). The four panels on the left show the enlarged portions marked by I - V. The panels on the right are schematic representations of zebra patterns seen in the corresponding left-hand-side panels. The individual zebra stripes are shown as solid lines with slopes representing the frequency drifts of individual stripes. The vertical bars show the instant bandwidths of drifting stripes in their bright portions. The two horizontal dashed lines indicate the frequency range of SSRT receivers. Arabic numerals attached to solid vertical lines mark the maximum moments of sub-second pulses recorded by the SSRT.

Note that the superfine structure was also observed during two other events on 10 April 2010 and 5 January 2003.

The configuration of the flare could be determined using sequences of radio maps in intensity and polarization (Sych *et al.*, 2010). During the flare there were two polarized 17 GHz sources: a compact source (right-handed, R) near the N-spot and a region extending southwestward with opposite polarization (L) (Figure 4). The L-region exhibits two centers of brightness on the northern and southern halves. The northern source emerged near the S-polarity spot. The

position of the southern source corresponded to the S-polarity extension that was elongated southward as the active region developed.

The flare was consisted of two loop systems joining the R-polarization region and the two L-polarization centers. The existence of a shorter loop in the south is consistent with the peak position of the emission intensity at 17 GHz at the top of the loop. Between the footpoints of the longer and higher loop was located the region of flare emission at 5.7 GHz, which was extended around the photospheric magnetic neutral line. The zebra sources were in the coronal part of this loop system. The apparent sizes of the sources were close to the SSRT beam size; therefore, their true sizes were much less than $15''$. The degree of polarization of radio pulses was low and showed changing signs. The significant difference among individual zebra structures suggests that their sources were located in different magnetic loops.

All the events with zebra structures detected in the dynamic spectra in the frequency range of 4.5–7.5 GHz are listed in Table 1. In all the cases, the frequency range of the zebra structures was less than the dynamic range of the spectro-polarimeter. We selected those events with at least two simultaneous bright stripes varying identically with time. The absorption bands (between bright stripes) with the brightness temperature lower than the background one, which had been detected occasionally at lower frequencies, were not observed in these events (Slottje, 1981). The magnetic field strengths in the zebra-structure sources were estimated by using the potential field approximation, and are given for a number of events. For the zebra stripes recorded with SSRT the polarization degree was determined from the SSRT data; for other cases a similar procedure was applied to the NOAC data.

Among the sources presented in Table 1, the 5 January 2003 zebra structure stands out. This event exhibited four stripes separated uniformly in frequency and synchronously changing frequency drifts. The event was studied in detail by Altyntsev *et al.* (2005). A frequency gap between adjacent stripes corresponded to the cyclotron frequency in the source region. The emission from the compact zebra source was X-mode polarized up to 100% degree.

The stripes observed in the 10 April 2001 event were equally spaced in frequency within the measurement accuracy. The analysis of this event (Chernov *et al.*, 2006) has demonstrated, however, that the emission mechanism with the Bernstein modes is inapplicable in this event because the frequency gaps between the adjacent stripes were too small. In the other events, the frequency separation between the stripes was not uniform. Usually the observations showed no more than four stripes. In some cases, a time delay was seen between the two similar stripes. The characteristic parameters of zebra structures are summarized in Table 2.

4. Discussion and Conclusions

The observations of zebra structures with high spatial resolution have revealed that their sources are located in the coronal part of flare loops in which the magnetic field does not exceed several hundred G. The narrow frequency bandwidth

Table 1. Parameters of zebra-patterns in six events.

Event	10 Apr 01 ¹			21 Aug 02	17 Sep 02		05 Jan 03 ²		18 Mar 03 ³	29 May 03 ⁴				
Number of stripes	4	2	2	2	2	2	4	4	4	3	3	3	2	3
Δf [GHz]	0.09– 0.2	0.11	0.12– 0.24	0.63– 0.73	0.44– 0.50	0.20– 0.38	0.16	0.22	0.3– 0.5	0.14– 0.48	0.23– 0.27	0.14– 0.27	0.13– 0.29	0.14– 0.21
Durations [s]	1.2	0.8	2.1	0.9	1.3	0.4	2.4	4.1	0.4	0.09	0.45	0.3	0.8	0.34
Instant stripe width, [GHz]	0.1	0.04	0.35	0.26	0.2	0.09	0.06	0.26	0.12– 0.29	0.04– 0.2	0.1– 0.16	0.16– 0.32	0.12– 0.16	0.1– 0.17
Drift rate, [GHz s ^{−1}]	−1.0 +0.2	−1.4 +0.6	−0.3 +1.0	+2.5	−1.0 +1.8	+2.7	−0.7 −0.5		−11. +19.6	+3.4 +4.9	+2.1 +2.7	+2.85 +3.23	+0.39 +0.44	+1.27 +1.81
Delay [ms]	<40	<10	<10	50	85		<10		10– 130					
Polarization [%]	30– 50	30– 50		5– 30		0	100	100	20	5	90	50	50	50

¹ Chernov *et al.* (2006)² Altyntsev *et al.* (2006)³ Ning *et al.* (2007)⁴ Sych *et al.* (2010)

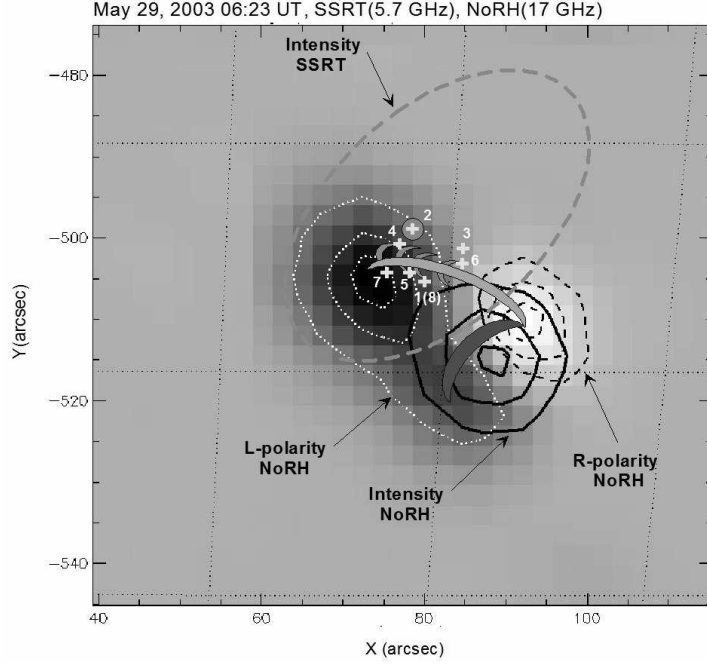


Figure 4. The positions of the radio sources at 5.7 GHz (SSRT) and 17 GHz (NoRH) superimposed on the radio map at 17 GHz in polarization at 02:13:00 UT, 29 May 2003. The white region corresponds to right circular polarization at 17 GHz. Brightness of this source is shown by the dashed contours at 20, 50, and 80% of the maximum brightness (0.2 MK). The white dotted contours (20, 50, and 80% of the minimum brightness (-0.58 MK) show the structure of the background L-source. Solid black contours indicate 20, 50, and 80% of the maximum brightness (15.8 MK) of the 17 GHz source in intensity (R+L). The grey thick dashed contour marks 20% of the maximum brightness of the 5.7 GHz source (12 MK) at 02:17:54.8 UT. The pluses (+) indicate the positions of zebra sources 1–8.

of zebra-structure stripes suggests a coherent mechanism for their generation. The coherent mechanism responsible for the continuous background emission will be characterized by the Langmuir frequency f_p determined by the plasma density n , and by the electron cyclotron frequency f_B which depends on the magnetic field strength B . The Langmuir frequency exceeds 4 GHz at a plasma

Table 2. The observed characteristics of zebra structures

Frequency range f [GHz]	5.2 – 7.5
Number of stripes	2 – 4
Frequency gaps between stripes Δf [GHz]	0.1 – 0.7
Duration [s]	0.1 – 4.1
Instant frequency width of a stripe [GHz]	0.04 – 0.35
Drift rate [GHz s ⁻¹]	0.4 – 19
Polarization [%]	0 – 50
Delay Δt [ms]	< 130

density of $2 \times 10^{11} \text{cm}^{-3}$. If the electromagnetic wave is emitted at twice the Langmuir frequency, the density in the source is about $5 \times 10^{10} \text{cm}^{-3}$. The cyclotron frequency reaches this value in the magnetic field over 1400 G (characteristic for flare loop footpoints in the chromosphere) while in the corona the magnetic field is much weaker. Hence, in the zebra sources the condition $f_p \gg f_B$ can be considered fulfilled.

In the events with simple configuration (17 September 2002 and 5 January 2001) with one flare loop, the GOES soft X-ray observations enabled us to estimate the plasma density in the source region. We found that the zebra frequencies were about twice the Langmuir frequency there. The coherent emission is caused by nonthermal electrons with pitch-angle anisotropy which will relax into equilibrium through excitation of electrostatic oscillations due to the development of loss-cone instability. In flare loops the electron beams with transverse anisotropy in the velocity distribution were observed by Altyntsev *et al.* (2007, 2008).

The first microwave zebra was found in the dynamic spectra of the flare of 5 January 2003 and described in Altyntsev *et al.* (2005). The frequency gap between adjacent bright stripes was constant and close to the cyclotron frequency. The SSRT observations revealed that there is only one emission source for multiple zebra stripes in the compact region. The position of the source relative to the magnetic field and the sense of polarization suggests the extraordinary mode of emission. The plasma density in the zebra source was estimated from soft X-ray data. The knowledge of plasma parameters in the source allowed us to identify the observed emission as the excitation of the Bernstein modes of magnetized plasma oscillations, namely the field-aligned electrostatic waves at harmonic frequencies of the cyclotron frequency (Altyntsev *et al.*, 2005; Kuznetsov, 2005).

In other events with three or four stripes, the zebra stripes were not equally-spaced in frequency. In this case, the most probable mechanism for generating zebra emission is the so-called double plasma resonance (DPR) (Zheleznyakov and Zlotnik, 1975; Zlotnik *et al.*, 2009). These individual stripes are assumed to be generated in different flare sites near the so-called resonance surfaces. On these surfaces the condition $f^s = \sqrt{f_p(n^s)^2 + f_B(B^s)^2} = s f_B(B^s)$ should be met, where n^s is the plasma density and B^s is the magnetic field strength on the resonance surface corresponding to the s -th harmonic. Under such condition the growth rate γ of the kinetic instability of upper hybrid waves is large, $\gamma \sim \frac{n_{ac}}{n} f_B$, and is much higher than the growth rate of the Bernstein-mode instability, where n_{ac} is the density of accelerated electrons.

The analysis of zebra characteristics in a meter-wave range has supported the DPR emission model (Aurass *et al.*, 2003; Zlotnik *et al.*, 2003). The 25 October 1994 event in AR 7792 with two interacting loops with scales differing by an order of magnitude has been examined. The magnetograms of this active region were used to calculate the magnetic field distribution along a large coronal loop. These calculations and zebra frequency structure have led to the plasma density distribution along the loop, which proved to be close to the expected hydrostatic distribution at a reasonable value of coronal plasma temperature of one million degrees.

The frequency gap in emission from different resonance surfaces should be equal: $\Delta f = 2f^{(s+1)} - 2f^s$. If $f_p \gg f_B$, the plasma density and the magnetic field strength in the sources of adjacent stripes are related as follows:

$$\frac{B^{(s+1)}}{B^s} = \frac{s}{s+1} \left(1 + \frac{\Delta f}{2f^s} \right) \quad (1)$$

$$\frac{n^{(s+1)}}{n^s} = \left(1 + \frac{\Delta f}{2f^s} \right)^2 \quad (2)$$

In the 17 September 2002 event, the estimated magnetic field strength is 200 G and the corresponding cyclotron frequency is 0.56 GHz. The frequency of the zebra structure may be as high as 6.4 GHz. If the transformation into electromagnetic waves occurs at twice the cyclotron frequency, then we obtain $s \approx 5$. Given the difference in frequencies between stripes $\Delta f = 0.44 \text{ GHz} \leq f_B$, we obtain the relations $\frac{B^{(s+1)}}{B^s} \approx 0.94$ and $\frac{n^{(s+1)}}{n^s} \approx 1.07$ between the magnetic field strength and plasma density in the sources of the stripes. It is evident that, in the case of small harmonic numbers, the changes in the magnetic field strength and density in the sources of adjacent stripes have opposite signs.

In the DPR model, the resonance conditions are determined by the magnetic field strength and plasma density, which can change with magnetohydrodynamic velocities and lead to the frequency drift of zebra stripes. The appearance and lifetime of zebra structures depend on the presence of nonthermal electrons with pitch-angle anisotropy in the resonance regions. A theoretical study on the excitation of zebra structure shows their critical dependence on the velocity and angular distributions of nonthermal electrons (see Zlotnik *et al.*, 2009). The mechanism of how DPR is generated under the condition of parameters close to the microwave observations with SSRT was examined in detail by Kuznetsov (2005, 2007, 2008) and Kuznetsov and Tsap (2007). Given a plasma temperature of about ten MK in a flare, the growth rate of loss-cone instability exceeds the Coulomb collision time if the nonthermal electron density satisfies $\frac{n_{ac}}{n} > 10^{-6}$. The theoretical analysis suggests that the intensity and the polarization degree of the emission may vary in a wide range and take the maximal values in a narrow angular range perpendicular to the magnetic field. The strong angular dependence of emission intensity is one of the reasons why they are so rarely observed.

Zebra structures were observed both in the disk center and near the limb. Therefore, the position of the source is supposed to be near the top of the flare loop where the density gradient along the loop is small. However, the DPR model with radio sources distributed along the loop requires higher density gradient as compared to the hydrostatic value (Chernov *et al.*, 2006). Figure 5 gives an example of how the location of the resonance surface is calculated. The calculations were made on the assumption that the frequency is doubled during the transformation of electrostatic oscillations into electromagnetic waves. The profile of the magnetic field along the loop is described by $B(h) = B_{\text{top}} \left(1 + \left(\frac{h}{L_B} \right)^2 \right)$

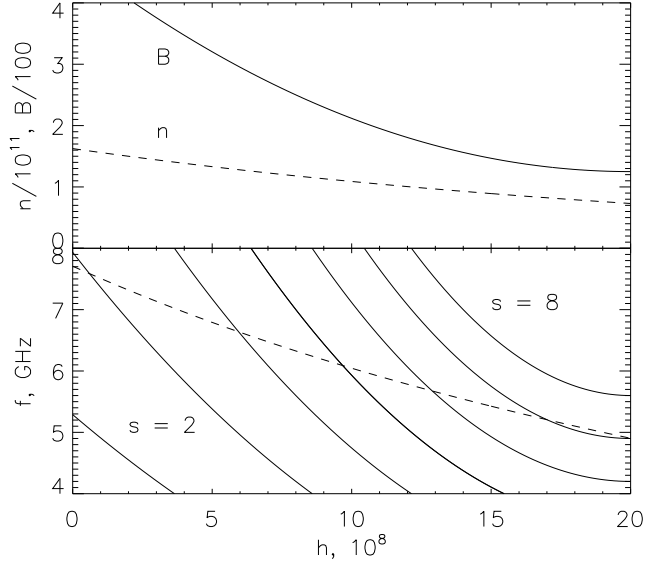


Figure 5. Top: Plasma density and magnetic field strength as a function of height. Bottom: Harmonics of the doubled cyclotron frequency (solid lines) and the upper-hybrid frequency (dashed line). The fifth cyclotron harmonic is shown by the thick solid curve.

(Lee and Gary, 2000). The graph for $B(h)$ in the upper panel of Figure 5 was derived by assuming $B_{\text{top}} = 125$ G and $L_B = 12$ Mm which are typical for flare loops. In the lower panel of Figure 5, the solid lines indicate the doubled frequencies of cyclotron harmonics in the range $s = 2 - 8$. The dashed lines show the plasma density (upper panel) and the doubled upper-hybrid frequency (lower panel) vs. height. The intersections of the dashed line with the solid curves in the lower panel of Figure 5 correspond to the resonance frequencies and their positions along the flare loop. The intersection of the upper-hybrid frequency (derived from the assumption of hydrostatic density distribution) and the fifth harmonic of the cyclotron frequency gives the frequency of 6.4 GHz, and the frequency gaps Δf are comparable to the observed ones as has been assumed. The simulation, however, shows that the plasma temperature (≤ 0.5 MK) in the loop should be several times lower than that of an ordinary coronal loop and by an order of magnitude lower than those characteristic of the flare plasma.

The frequency drift of brightness stripes in zebra structures reflects changes in plasma parameters in the source region. In order to retain the resonance, the equality between the Langmuir frequency and the cyclotron frequency harmonic requires a correlated temporal changes in plasma and magnetic field parameters as $n \sim B^2$. Such a relation between density and magnetic field is typical of the transverse equilibrium of a current rope. Let us consider the simplest case of a static magnetic tube in which the radial equilibrium condition $\frac{B^2(r)}{8\pi} + 2k_B n(r)T = \frac{B_{\text{ext}}^2}{8\pi}$ is met, where k_B is the Boltzmann constant and B_{ext} is the external magnetic field. It is assumed that plasma pressure can be

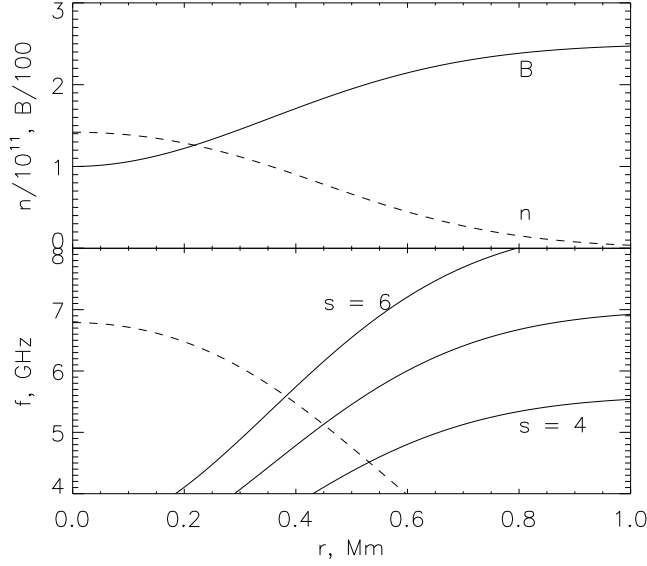


Figure 6. Similar to Figure 5 but for an equilibrium magnetic flux tube.

ignored outside the loop. Figure 6 presents the calculation results for this model analogous to those in Figure 5. The plasma temperature inside the tube is taken to be constant and equal to 8 MK. The radial magnetic field distribution is assumed to be $B=250-150 \exp(-r^2/p^2)$ [G], and the plasma density distribution is determined from the equilibrium equation. The scale p in the magnetic field is a free parameter and it is taken as 0.5 Mm.

Thus, a simple model with reasonable assumptions about plasma parameters can satisfactorily describe the observed frequency gaps between zebra stripes (Figure 7). The frequency gaps will be higher than the cyclotron frequency at small harmonic numbers and lower at large harmonic numbers. The model has a number of free parameters such as the radial profile of magnetic field and plasma temperature. By choosing these parameters, we can obtain agreement between the calculated and observed zebra structures. It seems reasonable to attribute the frequency drift of zebra stripes to sausage oscillations which generate an increase of plasma density and magnetic field in compressible magnetic tubes. The observed frequency range of about 1 GHz is achieved for a relatively small change in plasma density ($\approx 30\%$).

In order to explain the narrow frequency band of a single strip, the longitudinal size of the emitting region should be much less than the characteristic scales of plasma density and magnetic field variations. The upper bound on the size of the emitting region can be estimated considering the absorption of electromagnetic waves in the plasma surrounding the magnetic tube. According to Benz *et al.* (1992) the optical thickness at twice the Langmuir frequency is $\tau = 1.2 T_{\text{keV}}^{-3/2} \nu_{\text{GHz}}^2 \lambda_{\text{cm}}$, where λ is the radial scale of density variations. At $\lambda = 0.5$ Mm, we obtain $\tau \approx 0.1$, and the absorption when the emission

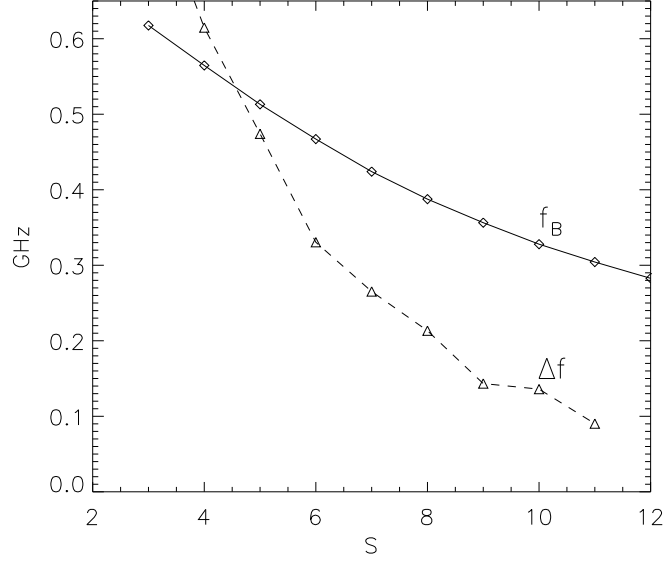


Figure 7. The calculated frequency gaps between adjacent strips (dashed line) in comparison with the cyclotron frequency on the corresponding surfaces (solid curve).

escapes across the magnetic tube is negligible. However, the absorption may be substantial if the loop radius is more than several thousand kilometers and the emission is observed in the direction along the loop.

The superfine structures observed in the three zebra events are not the main subject of this study. Observations of such structures were described by Chernov *et al.* (1998); Chernov (2003); Meszarosova *et al.* (2008). Kuznetsov (2008) and Rozhansky *et al.* (2008) have concluded that superfine temporal structures are formed due to modulation of the emission mechanism by MHD turbulence in the zebra sources. To promote understanding of the phenomena we will be able to exclude the propagation effects by conducting simultaneous observations using multiple radio telescopes. There is only 10 April 2001 event which was observed simultaneously with the PMO and the Huairou station. In Figure 2 of Chernov *et al.* (2006) all smooth changes in the zebra stripes were strictly identically reproduced in the spectra from both observatories, but there was no detailed correspondence between the fine structures of the stripes.

Up-to-date high-sensitivity spectro-polarimeters enabled us to record several events with microwave zebra structures. Among two hundred events with fine time structures recorded by Chinese spectro-polarimeters and SSRT in the frequency range from 5.2 to 7.5 GHz, only six events had zebra structures. Their intensity did not exceed several solar flux units. The observed stripes in the microwave range corresponded to small numbers of harmonics— near the fifth—, and there were no more than four stripes simultaneously. The frequency gaps between adjacent stripes varied over a wide range from 0.1 to 0.7 GHz. The characteristics of the observed events are consistent with our knowledge about

the emission mechanism (the double plasma resonance) and can be applied to the diagnostics of plasma conditions in coronal flare loops.

Acknowledgement

We appreciate discussions with Dr. E.Ya. Zlotnik. The research carried out by Robert Sych at NAOC was supported by the Chinese Academy of Sciences Visiting Professorship for Senior International Scientists, grant No. 2010T2J24. This study was supported by the Russian Foundation of Basic Research (08-02-00270, 08-02-92204-GFEN, 09-02-92610, 09-02-00226, 10-02-00153a). This research was supported by a Marie Curie International Research Staff Exchange Scheme Fellowship within the 7th European Community Framework Programme.

References

- Altyntsev, A.T., Grechnev, V.V., Kononov, S.K., Lesovoi, S.V., Lisysian, E.G., Treskov, T.A., Rosenraukh, Yu.M., Magun, A.: 1996, *Astrophys. J.* **469**, 976.
- Altyntsev, A.T., Lesovoi, S.V., Meshalkina, N.S., Sych, R.A., Yan, Y.: 2003, *Astron. Astrophys.* **400**, 337.
- Altyntsev, A.T., Kuznetsov, A.A., Meshalkina, N.S., Rudenko, G.V., Yan, Y.: 2005, *Astron. Astrophys.* **431**, 1037.
- Altyntsev, A.T., Grechnev, V.V., Meshalkina, N.S., Yan, Y.: 2007, *Solar Phys.* **242**, 111.
- Altyntsev, A.T., Fleishman, G. D., Huang, G.-L., Melnikov, V. F.: 2008, *Astrophys. J.* **677**, 1367.
- Aurass H., Klein K.-L., Zlotnik E.Ya., Zaitsev V.V.: 2003, *Astron. Astrophys.* **410**, 1001.
- Benz, A.O., Magun, A., Stehling, W., Su, H.: 1992, *Solar Phys.* **141**, 335.
- Chernov, G.P., Markeev, A.K., Poquérusse, M., Bougeret, J.L., Klein, K.-L., Mann, G., Aurass, H., Aschwanden, M.J.: 1998, *Astron. Astrophys.* **334**, 314.
- Chernov, G.P., Yan, Y.H., Fu, Q.J.: 2003, *Astron. Astrophys.* **406**, 1071.
- Chernov, G.P.: 2006, *Space Sci. Rev.* **127**, 195.
- Chernov, G.P., Sych, R.A., Yan, Y., Fu, Q., Tan, C., Huang, G., Wang, De-Yu, Wu, H.: 2006, *Solar Phys.* **237**, 397.
- Grechnev, V.V., Lesovoi, S.V., Smolkov, G.Y., Krissinel, B.B., Zandanov, V.G., Alyntsev, A.T., et al.: 2003, *Solar Phys.* **216**, 239.
- Fu, Q., Qin, Z., Ji, H., Pei, L.: 1995, *Solar Phys.* **160**, 97.
- Handy, B. N., Acton, L. W., Kankelborg, C. C., Wolfson, C. J., Akin, D. J., Bruner, M. E., et al.: 1999, *Solar Phys.* **187**, 229.
- Ji, H., Fu, Q., Liu, Y., Cheng, C., Chen, Z., Yan, Y., Zheng, L., Ning, Z., Tan, C., Lao, D.: 2003, *Solar Phys.* **213**, 359.
- Kuznetsov, A.A.: 2005, *Solar Phys.* **438**, 341.
- Kuznetsov, A.A.: 2007, *Plasma Phys. Rep.* **33**, 482.
- Kuznetsov, A.A., Tsap, Y.T.: 2007, *Solar Phys.* **241**, 127.
- Kuznetsov, A.A.: 2008, *Solar Phys.* **253**, 103.
- Lee, J., Gary, D.E.: 2000, *Astrophys. J.* **543**, 457.
- Lesovoi, S.V., Kardapolova, N.N.: 2003, *Solar Phys.* **216**, 225.
- Lin, R.P., Dennis, B.R., Hurford, G.J., Smith, D.M., Zehnder, A., Harvey, P.R., et al.: 2002, *Solar Phys.* **210**, 3.
- Meszarosova, H., Karlický, M., Sawant, H. S., Fernandes, F. C. R., Cecatto, J. R., de Andrade, M. C.: 2008, *Astron. Astrophys.* **491**, 555.
- Nakajima, H., Sekiguchi, H., Sawa, M., Kai, K., Kawashima, S.: 1985, *Pub. Astron. Soc. Japan* **37**, 163.
- Nakajima H., Nishio, M., Enome, S., Shibasaki, K., Takano, T., Hanaoka, Y., et al.: 1994, *Proc. IEEE* **82**, 705.
- Ning Z., Wu H., Xu F., Meng X.: 2007, *Solar Phys.* **242**, 101.

- Ramaty, R.: 1969, *Astrophys. J.* **158**, 753.
- Ramaty, R., Schwartz, R. A., Enome, S., Nakajima, H.: 1994, *Astrophys. J.* **436**, 941.
- Rozhansky, I. V., Fleishman, G. D., Huang, G.-L.: 2008, *Astrophys. J.* **681**, 1688.
- Scherrer, P. H., Bogart, R. S., Bush, R. I., Hoeksema, J. T., Kosovichev, A. G., Schou, J., *et al.*: 1995, *Solar Phys.* **162**, 129.
- Slottje, C.: 1981 *Atlas of Fine Structures of Dynamic Spectra of Solar Type IV -dm and Some Type II Bursts*, Utrecht Observatory.
- Sych, R.A., Chernov, G.P., Altyntsev, A.T., Meshalkina, N.S., Yan, Y., Tan, C.: 2010, 38th COSPAR Scientific Assembly, paper number E25-0080-10.
- Torii, C., Tsukiji, Y., Kobayashi, S., Yoshimi, N., Tanaka, H., Enome, S.: 1979, *Proc. Res. Inst. Atmospheric, Nagoya Univ.*, **26**, 129.
- Zheleznyakov, V.V., Zlotnik, E.Ya.: 1975, *Solar Phys.* **44**, 461.
- Zlotnik, E.Ya., Zaitsev, V.V., Aurass, H., Mann, G., Hofmann, A.: 2003, *Astron. Astrophys.* **410**, 1011.
- Zlotnik, E.Ya., Zaitsev, V.V., Aurass, H., Mann, G.: 2009, *Solar Phys.* **255**, 273.
- Zlotnik, E.Ya.: 2011, *Solnechno-Zemnaya Fizika, Irkutsk* **16**, 49.

